of adult HSCs [13]. Furthermore, VEGF has been shown to be an essential factor for HSC niche formation through endochondral ossification [14]. These observations clearly demonstrate that VEGF exerts physiological actions on hematopoietic systems through both cell-autonomous and -nonautonomous mechanisms.

In addition to the functions described above, VEGF also has a potent HSPC mobilization capacity [15], although the mechanisms of VEGF-induced HSPC mobilization have not been addressed in detail. In the current study, we investigated the effect of VEGF on the BM cell mobilization and BM environment after the intravenous injection of VEGF-expressing adenovirus (Ad) vector (Ad-VEGF) into mice. The results showed that VEGF overexpression in mice could lead to a reduction of not only the HPSC number, but also the MPC number in the BM. We also observed an enhanced chemoattractive activity of BM stromal cells by VEGF. Our data suggest that the plasma elevation of VEGF in mice alters the distribution of MPCs in the BM, and this might cause HSPC egress from the BM.

Materials and Methods

Ad vectors

Ad vectors were constructed by an improved in vitro ligation method [16,17]. The mouse $VEGF_{165}$ cDNA and human G-CSF cDNA were obtained from pBLAST49-mVEGF and pORF9-hGCSFb, respectively (Invivogen). Each cDNA was cloned into a multicloning site of pHMCMV10 [18,19], which contains the cytomegalovirus (CMV) promoter/enhancer and intron A sequence flanked by the I-*Ceu*I and PI-*Sce*I sites, thereby resulting in pHMCMV10-VEGF and pHMCMV10-G-CSF. pHMCMV10-VEGF and pHMCMV10-G-CSF were digested with I-*Ceu*I/PI-*Sce*I and ligated into I-*Ceu*I/PI-*Sce*I-digested pAdHM41-K7 (C) [20], resulting in pAd-VEGF and pAd-G-CSF, respectively. To generate the virus, Ad vector plasmids were digested with *Pac*I and purified by phenol–chloroform extraction and ethanol precipitation. Linearized DNAs were transfected into 293 cells with SuperFect (Qiagen) according to the manufacturer's instructions. The viruses were amplified in 293 cells. Before virus purification, the cell lysates were centrifuged to remove cell debris and were digested for 30 min at 37°C with 200 μg/mL DNase I and 200 μg/mL RNase A in the presence of 10 mM $MgCl_2$. Viruses were purified by $CsCl_2$ step gradient ultracentrifugation followed by $CsCl_2$ linear gradient ultracentrifugation. The purified viruses were dialyzed against a solution containing 10 mM Tris-HCl (pH 7.5), 1 mM $MgCl_2$, and 10% glycerol and were stored at −80°C. The control vector, Ad-Null, is similar in design, except that it contains no transgene in the expression cassette. The biological titers [infectious unit (ifu)] of Ad-VEGF, Ad-G-CSF, and Ad-Null were determined by using an Adeno-X Rapid Titer kit (Clontech).

Administration of Ad vectors in mice

C57BL/6j female mice aged 7–9 weeks were obtained from Nippon SLC, and all animals were maintained under specific pathogen-free conditions. Each Ad vector was intravenously injected into C57BL/6j mice at 1×10^9 ifu through the tail vein. All experiments were conducted according to the institutional ethics guidelines for animal experimentation of the National Institute of Biomedical Innovation.

Cell preparation

Blood and BM were harvested from mice using standard methods on day 5 after injection of Ad vector into mice, and the number of nucleated cells in these tissues was then counted using a Nucleocounter (Chemometec). To collect the nonhematopoietic cells from the femur and tibia, the bone fragments were minced with scissors, and were then incubated at 37°C with a type I collagenase (3 mg/mL; Worthington) in the Dulbecco's modified Eagle's medium (DMEM) with 10% fetal bovine serum (FBS) for 90 min [21]. The cells were filtered with a cell strainer to remove debris and bone fragments, and suspended in a staining buffer [phosphate buffer saline (PBS)/2% FBS]. These cell suspensions were kept on ice for further analysis.

Flow cytometry

The following antibodies (Abs), conjugated with fluorescein isothiocyanate (FITC), phycoerythrin (PE), allophycocyanin (APC), or PECy7, were used for flow cytometric analysis and cell sorting: biotinylated lineage cocktail [CD3 (145-2C11), B220 (RA3-6B2), Gr-1 (RB6-8C5), CD11b (M1/70), Ter119 (Ter-119)], c-Kit-APC (2B8), Sca-1-PECy7 (D7), Ter119-FITC (Ter-119), CD45-FITC (30-F11), CD11b-FITC (M1/70), Gr-1-PE (RB6-8C5), CD31-FITC (390), CD31-APC (390), CD51-PE (RMV-7), PDGFRa-APC (APA-5), Flt-1-PE (141522), Flk1-PE (Avas12a1), and Alcam-PE. For detection of biotinylated Abs, PerCP-Cy5.5- or FITC-conjugated streptavidin was used. Abs were purchased from e-Bioscience, BD Bioscience, Biolegend, and R&D Systems. Cells were incubated with primary Abs at 4°C for 30 min and washed twice with PBS/2% FBS. After staining, cells were analyzed and isolated by flow cytometry on an LSR II and FACSAria flow cytometer, respectively, using FACSDiva software (BD Bioscience).

Enzyme linked immunosorbent assay

Blood samples were collected through the inferior vena cava on day 5 after Ad vector injection, and transferred to polypropylene tubes containing heparin. Plasma was harvested by centrifugation. The BM supernatant was obtained by flushing a femur with 500 μL of PBS, followed by centrifugation at 500*g* for 5 min. The levels of VEGF and CXCL12 in the plasma and BM supernatant were measured using a commercial ELISA kit (R&D Systems) following the manufacturer's instructions.

Reverse transcription-polymerase chain reaction analysis

CD45-negative($^-$) $Ter119^-$ nonhematopoietic cells in the BM were sorted from mice injected with Ad-VEGF or Ad-Null, and total RNA was then extracted using ISOGEN (Nippon Gene). cDNA was synthesized from DNase I-treated total RNA with a Superscript VILO cDNA synthesis kit

(Invitrogen), and quantitative real-time reverse transcription-polymerase chain reaction was performed using the Fast SYBR Green Master Mix with an ABI StepOne Plus system (Applied Biosystems). Relative quantification was performed against a standard curve and the values were normalized against the input determined for the housekeeping gene, glyceraldehyde 3-phosphate dehydrogenase. The sequences of the primers used in this study are listed in Table 1.

Colony assay

BM cells (2×10^4 cells) and peripheral blood cells (2×10^5 cells) were plated in the Methocult M3434 medium (StemCell Technologies, Inc.). Cultures were plated in duplicate and placed in a humidified chamber with 5% CO_2 at 37°C for 10 days. The number of individual colonies was counted by microscopy. The colony number was normalized to the total number of the nucleated cells.

Colony forming unit-fibroblast assay

BM-derived $CD45^-Ter119^-$ cells were added to the MesenCult MSC Basal Medium, including supplements (Stem Cell Technologies, Inc.), and then plated on a six-well plate at 1×10^5 cells per well. Cells were cultured for 14 days and stromal cell colonies (fibroblast-like colonies: >50 cells) derived from colony forming unit-fibroblasts (CFU-Fs) were stained with the Giemsa solution (Wako) after fixation with methanol. The colony number was counted by microscopy.

Cell migration assay

BM-derived stromal cells, including MPCs, were tested for migration toward VEGF using 8-μm pore-sized cell culture inserts (BD Falcon). Stromal cells (1×10^5 cells) resuspended in 200 μL of DMEM/2% FBS were added to the upper chamber, and 750 μL of DMEM/2% FBS containing recombinant mouse VEGF (10 or 100 ng/mL; Peprotech) was added to the bottom chamber. After 6 h of incubation at 37°C, the upper side of the filters was carefully washed with PBS, and cells remaining on the upper face of the filters were removed with a cotton wool swab. The filters were fixed with 100% methanol and stained with the Giemsa solution. Cells migrating into the lower compartment were counted manually in three random microscopic fields (×200).

Homing assay

Mice were administrated with Ad-Null or Ad-VEGF at 1×10^9 ifu. Five days later, BM cells (1×10^7 cells) derived from green fluorescent protein (GFP)-expressing transgenic mice [22] were intravenously transplanted into Ad-Null- or Ad-VEGF-injected mice. At 16 h after BM transplantation, the percentage of GFP-expressing donor cells in the BM was determined by flow cytometry.

Results

Effect of systemic VEGF overexpression on the distribution of myeloid cells and HSPCs in mice

To evaluate the effect of VEGF on the mobilization of hematopoietic cells, we generated a VEGF-expressing Ad vector, Ad-VEGF, because plasma VEGF levels were rapidly decreased with a $t_{1/2}$ of ~25 min after intravenous injection of recombinant VEGF [23]. Single intravenous injection of Ad-VEGF (1×10^9 ifu) into mice led to a significant elevation of VEGF levels in plasma on day 5 compared with Ad-Null-injected mice (control mice) (Fig. 1a). On the other hand, unexpectedly, BM VEGF levels in the Ad-VEGF-injected mice were almost equivalent to those in the Ad-Null-injected mice (Fig. 1b). There were no signs of toxicity in mice treated with Ad-VEGF and Ad-Null at this dose (1×10^9 ifu). To investigate whether the hematopoietic cells could be mobilized from the BM into the circulation after injection of Ad-VEGF, we examined the number of total nucleated cells, myeloid cells ($Gr\text{-}1^+CD11b^+$ cells), and HSPCs [$c\text{-}Kit^+Sca\text{-}1^+Lineage^-$ (KSL) cells or CFU-granulocyte, erythroid, macrophage, megakaryocyte/CFU-Mix] in the peripheral blood. Compared with Ad-Null-injected mice, Ad-VEGF-injected mice showed an increased number of total nucleated cells and myeloid cells in the peripheral blood (Fig. 1c, d). We found that the number of multipotent hematopoietic progenitor cells, CFU-GEMM/CFU-Mix, in the blood of Ad-VEGF-injected mice was four times as great as that of Ad-Null-injected mice (Fig. 1e). Importantly, in Ad-VEGF-injected mice, the number of KSL cells in the blood was also increased (Fig. 1f). These results indicate that hematopoietic cells, including immature hematopoietic cells with colony-forming potentials, would be mobilized from the BM following systemic Ad-VEGF administration.

An increased number of mobilized cells in VEGF-treated mice were reported previously [15], but little is known about the effect of VEGF on BM cells during the mobilization period. Thus, we next investigated the number of total BM cells, myeloid cells, and HSPCs. In contrast to the peripheral blood, the number of total hematopoietic cells, myeloid cells, and CFU-Mix was significantly decreased (Fig. 2a–c). It is of note that the VEGF overexpression in mice resulted

Table 1. Primer Sequences Used in this Study

Gene name	*(5′) Sense primers (3′)*	*(5′) Antisense primers (3′)*
Gapdh	TTCACCACCATGGAGAAGAAGGC	GGCATGGACTGTGGTCATGA
Cdh2	CAAGAGCTTGTCAGAATCAGG	CATTTGGATCATCCGCATC
Vcam-1	GACCTGTTCCAGCGAGGGTCTA	CTTCCATCCTCATAGCAATTAAGGTG
Angpt1	CTCGTCAGACATTCATCATCCAG	CACCTTCTTTTAGTGCAAAGGCT
Thpo	GGCCATGCTTCTTGCAGTG	AGTCGGCTGTGAAGGAGGT

Gapdh, glyceraldehyde 3-phosphate dehydrogenase; *cdh2*, N-cadherin; *Vcam-1*, vascular cell adhesion molecule-1; *Angpt1*, angiopoietin-1; *Thpo*, thrombopoietin.

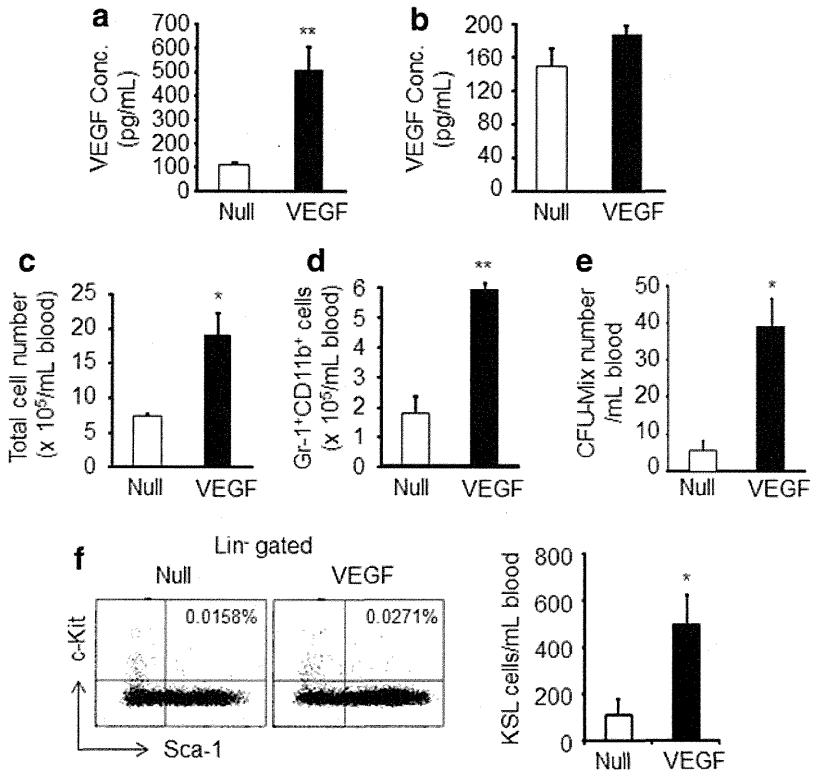

FIG. 1. Effect of vascular endothelial growth factor (VEGF) on the number of myeloid cells and hematopoietic stem/progenitor cells (HSPCs) in peripheral blood. **(a, b)** Mice were intravenously injected with adenovirus (Ad)-Null (Null) or Ad-VEGF (VEGF). Five days later, the concentration of plasma **(a)** and bone marrow (BM) **(b)** VEGF levels was determined by enzyme linked immunosorbent assay (ELISA). Data are expressed as mean ± standard deviation (SD) ($n=4$). **(c)** The number of total peripheral blood mononuclear cells (PBMCs) was counted on day 5 after administration of each Ad vector. **(d)** The percentage of Gr-1$^+$CD11b$^+$ myeloid cells was determined by flow cytometric analysis, and the absolute number was then normalized to the total PBMC number. Data are expressed as mean ± SD ($n=4$). **(e)** The number of colony forming unit (CFU)-Mix/CFU-granulocyte, erythroid, macrophage, megakaryocyte (GEMM) a multipotent hematopoietic progenitor cells, in PBMCs was determined by a standard colony assay. The colony number was normalized to the total PBMC number. **(f)** A representative analysis of the c-Kit$^+$Sca-1$^+$Lineage$^-$(KSL) subset in the blood is shown (*left*). The proportion of cKit$^+$Sca-1$^+$ cells in the lineage-negative (Lin$^-$) population is indicated in the dot blot. The number of KSL cells in the blood was normalized to the total cell number (*right*). Data are expressed as mean ± SD ($n=4$). *$P<0.05$, **$P<0.01$ as compared with Null.

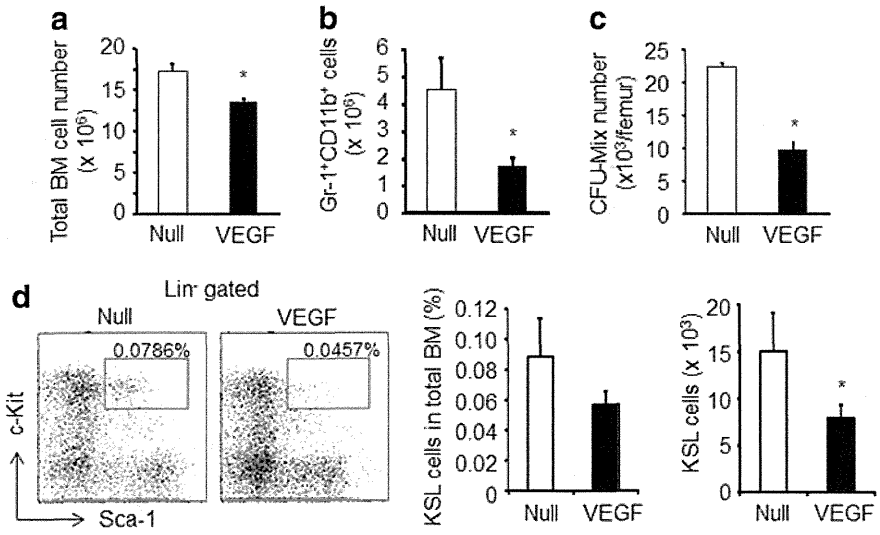

FIG. 2. Plasma elevation of VEGF leads to a decrease in the myeloid cells and HSPCs in the BM. **(a)** The number of total BM cells was counted on day 5 after Ad-Null or Ad-VEGF injection. **(b)** The number of Gr-1$^+$CD11b$^+$ cells in the BM was determined by flow cytometric analysis. **(c)** The number of CFU-Mix/CFU-GEMM in the BM was determined by a colony assay. The colony number was normalized to the total BM cell number. **(d)** A representative analysis of the KSL subset in the BM after administration of Ad-Null or Ad-VEGF is shown (*left*). The proportion of KSL cells in the total BM is indicated in the dot blot. Frequencies (*middle*) and absolute numbers (*right*) of KSL cells in the BM were calculated. Data are expressed as mean ± SD ($n=5$). *$P<0.05$ as compared with Null.

in the reduction in both the frequency and the absolute number of KSL cells in BM (Fig. 2d). Thus, these data suggest that VEGF exerts a physiological effect on the various types of cells within the BM.

Unchanged level of CXCL12 after VEGF overexpression

To examine the mechanisms of BM cell mobilization by VEGF treatment, we analyzed the expression levels of genes associated with HSC maintenance in the BM [*N-cadherin* (*cdh2*), *vascular cell adhesion molecule-1* (*Vcam-1*), *angiopoietin-1* (*Angpt1*), and *thrombopoietin* (*Thpo*)]. The expression levels of these genes in BM nonhematopoietic cells were modestly downregulated after Ad-VEGF injection (Fig. 3a). We next measured the CXCL12 levels in Ad-VEGF-injected mice. Chemokine CXCL12 is an indispensable factor for the maintenance and retention of HSPCs in the BM [5,24]. Previous studies showed that the BM CXCL12 levels were reduced by the injection of mobilization-inducing factors, such as G-CSF and stem cell factor (SCF) [10,25]. We also found that the CXCL12 levels were markedly reduced in the BM, but not the plasma, of Ad-G-CSF-injected mice (Fig. 3b). However, there was almost no difference in the BM CXCL12 levels between Ad-VEGF-injected mice and Ad-Null-injected mice (Fig. 3b). Therefore, these data indicate that VEGF would alter the BM microenvironment, probably by a different mechanism from other mobilization factors.

Reduction of MPCs in the BM after Ad-VEGF injection

Recent studies have demonstrated that MPCs play a pivotal role in HSPC maintenance in the BM [4,6–8]. Therefore, we examined the disposition of MPCs in the BM after Ad-VEGF administration. Flow cytometric analysis of the enzymatically dissociated BM cells revealed that Ad-VEGF overexpression led to a significant reduction of $CD45^-Ter119^-CD31^-Alcam^-Sca\text{-}1^+$ cells, which are reported to be MPCs [21,26] (Fig. 4a). In addition, the percentage of other MPC populations, such as $CD45^-Ter119^-PDGFR\alpha^+Sca\text{-}1^+$ cells [27] and $CD45^-Lineage^-CD31^-CD51^+Sca\text{-}1^+$ cells [28], in the BM of Ad-VEGF-injected mice was also lower than those of Ad-Null-injected mice (Fig. 4b, c). These data clearly showed the decreased number of phenotypically identified MPCs in the BM after injection of Ad-VEGF.

Next, to investigate whether functional MPCs in the BM were reduced in Ad-VEGF-injected mice, we performed a CFU-F assay and homing assay. Consistent with the above data, we observed decreased CFU-F numbers in the BM in Ad-VEGF-injected mice (Fig. 4d). For homing studies, Ad-Null- or Ad-VEGF-injected mice were used as the recipient mice. Donor BM cells derived from GFP transgenic mice were intravenously injected into nonirradiated recipient mice, and the frequency of GFP-expressing cells in the recipient BM was then estimated by flow cytometry. The results showed that the homing activity of GFP-expressing cells was partially inhibited in Ad-VEGF-treated recipient mice (Fig. 4e). Thus, the decreased homing efficiency of donor HSPCs in Ad-VEGF-injected mice suggests the decreased number of niche cells in the BM. Taken together, our findings indicate that overexpression of VEGF in mice leads to a reduction of phenotypic and functional MPCs in the BM.

VEGF stimulates the migration of MPCs

We next examined the mechanisms of the reduction of MPCs in the BM after VEGF overexpression. In vitro-expanded primary mouse BM stromal cells (mBMSCs), including MPCs, showed slight expression of Flt-1 (VEGFR1), but not Flk-1 (VEGFR2), on the cellular surface (Fig. 5a). We speculated that MPCs might egress from the BM in response to the plasma level of VEGF, because there was almost no change in the BM VEGF levels in Ad-VEGF-injected mice (Fig. 1b). We performed an in vitro migration assay and found a dose-dependent chemoattractive effect of VEGF on mBMSCs (Fig. 5b), suggesting the possibility that a decreased number of BM MPCs in Ad-VEGF-injected mice would result from the mobilization of MPCs to the peripheral tissue in response to an elevation of plasma VEGF.

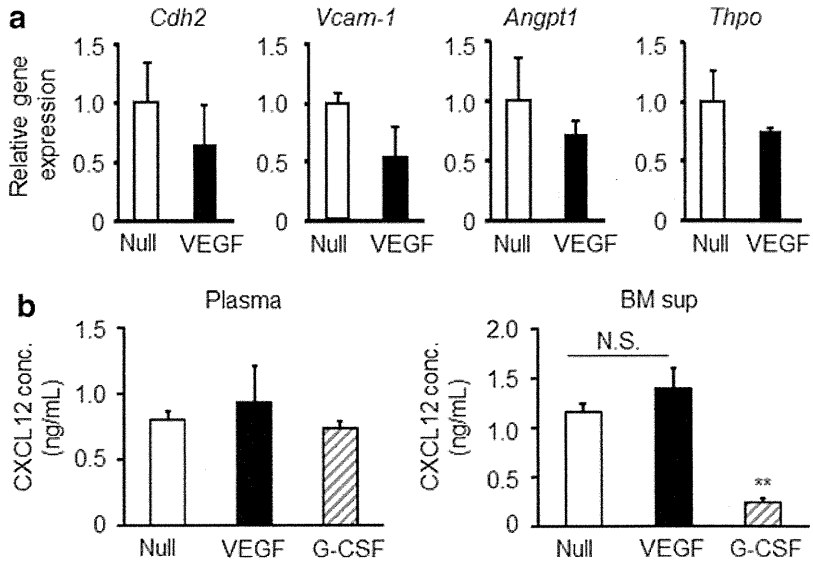

FIG. 3. Expression of HSPC maintenance factor genes after Ad-VEGF administration. **(a)** Expression levels of cadherin2 (Cdh2), vascular cell adhesion molecule-1 (Vcam-1), angiopoietin-1 (Angpt1), and thrombopoietin (Thpo) in nonhematopoietic cells ($CD45^-Ter119^-$ cells) were measured by quantitative polymerase chain reaction analysis. Data are expressed as mean ± SD ($n=3$). **(b)** The plasma and BM supernatants of mice injected with Ad-Null, Ad-VEGF, or Ad-GCSF were collected. The levels of CXC chemokine ligand 12 (CXCL12) in the plasma (*left*) and the BM supernatant (*right*) were measured by ELISA. $^{**}P<0.01$ as compared with Null. N.S. stands for not significant.

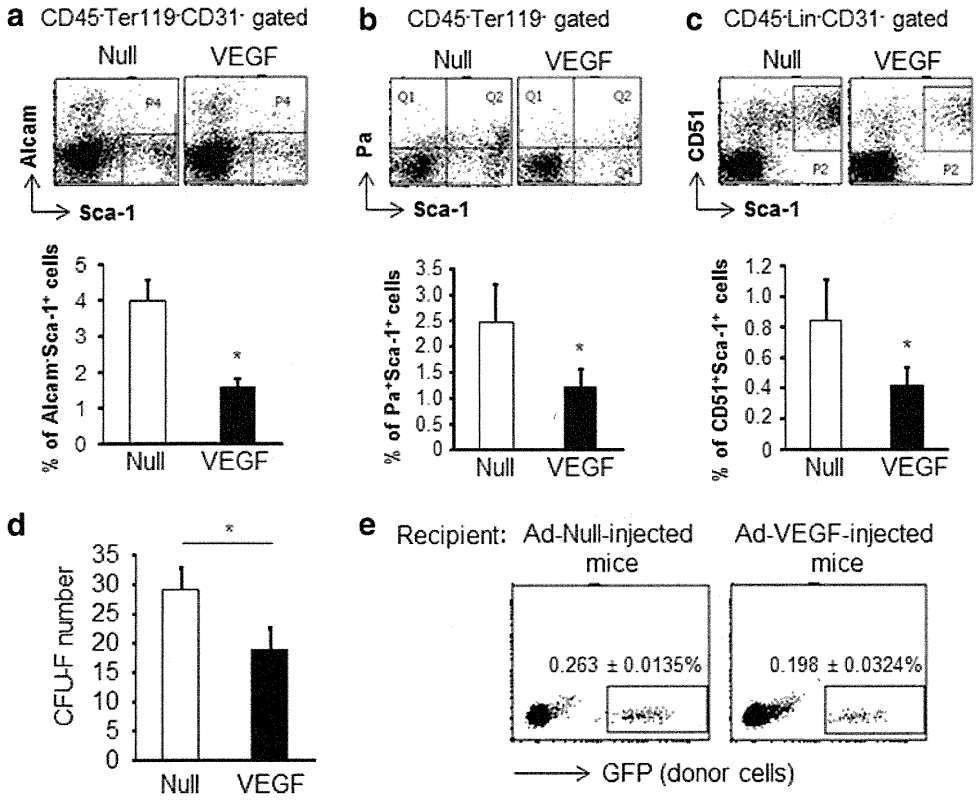

FIG. 4. The number of mesenchymal progenitor cells (MPCs) in the BM is decreased following Ad-VEGF injection. **(a–c)** After BM stromal cells were collected from bone by treatment with collagenase, the proportion of MPC populations [$CD45^-Ter119^-CD31^-Alcam^-Sca\text{-}1^+$ MPCs **(a)**, $CD45^-Ter119^-$ $PDGFRa^+$ (Pa^+) $Sca\text{-}1^+$ MPCs **(b)**, or $Lin^-CD45^-CD31^-CD51^+Sca\text{-}1^+$ MPCs **(c)**] in the BM was determined by flow cytometry. Data are expressed as mean ± SD ($n=5$). **(d)** A colony-forming unit-fibroblast (CFU-F) assay was performed using $CD45^-Ter119^-$ BM cells. The number of CFU-Fs was counted using a microscope after staining with the Giemsa solution. Data are expressed as mean ± SD ($n=3$). **(e)** Homing assay. After injection of Ad-Null or Ad-VEGF into mice, green fluorescent protein (GFP) transgenic mice-derived BM cells (donor cells) were transplanted into Ad vector-administrated mice. The percentage of donor cells (GFP-expressing cells) in the BM of Ad-Null- or Ad-VEGF-injected mice was analyzed by flow cytometry at 16 h after BM transplantation. The percentage of donor cells in the BM is indicated in the dot blot. Data are expressed as mean ± SD ($n=5$). $^*P<0.05$ as compared with Null.

Discussion

Recent studies have clearly reported that the HSPC numbers in the BM are significantly decreased by conditional deletion of MPCs, including nestin-expressing stromal cells [4] and CXCL12-abundant reticular cells [5]. It is of note that deletion of MPCs led to the increased number of HSPCs in the spleen, demonstrating the mobilization of HSPCs from BM to peripheral tissues [4]. Therefore, maintenance and retention of HSPCs in the BM would

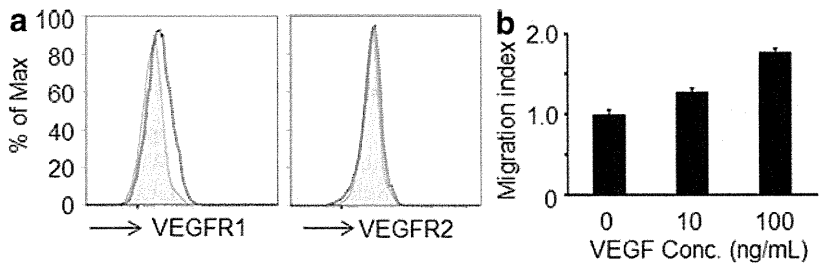

FIG. 5. VEGF enhances the migration capacity of MPCs. BM-derived stromal cells were collected and propagated in a tissue culture dish. **(a)** Expression levels of VEGF receptors, VEGFR1 (*left*) and VEGFR2 (*right*), in the cells was determined by flow cytometry. Staining profiles of specific mAb (*dotted lines*) and an isotype-matched control mAb (*gray area*) are shown. **(b)** BM stromal cells were exposed to various doses of recombinant VEGF. Cells that had migrated toward the VEGF (*lower chamber*) by passing through a membrane filter were counted by microscopy after staining with the Giemsa solution. Data are expressed as mean ± SD ($n=3$).

considerably be dependent on the number of MPCs [4,5]. In the present study, we examined the effect of VEGF on the disposition of BM HSPCs and MPCs in mice. Our main finding was that VEGF overexpression in mice resulted in a reduction of not only HSPCs but also MPCs in the BM. We also found that VEGF could promote the migration of mBMSCs in vitro. The data described here suggest that, as in the case of HSPCs, MPCs would also be mobilized to the peripheral tissues in response to an elevation of plasma VEGF levels, and a reduced number of BM MPCs by VEGF would lead to HSPC egress from the BM, because MPCs would function as niche cells in the BM.

It is well known that BM CXCL12 levels are down-regulated following G-CSF administration and thereby induce an egress of HSPCs [25,29]. Christopher et al. previously showed the reduced BM CXCL12 levels after administration of other mobilization factors, such as SCF and Flt3-ligand [10]. In addition to their mobilization-inducing effects, these factors also impact the number of stem and progenitor cells in the BM. For instance, it has been reported that the number of HSPCs and MPCs in the BM was significantly increased after G-CSF administration [30,31]. Unlike in the case of G-CSF and other mobilization factors, however, VEGF had almost no effect on BM CXCL12 levels (Fig. 3b). Furthermore, systemic VEGF expression resulted in a significant reduction in the number of HSPCs (KSL cells and CFU-Mix) in the BM (Fig. 2). The number of MPCs in the BM was also reduced in Ad-VEGF-injected mice (Fig. 4). Therefore, these data strongly indicate that VEGF would induce HSPC mobilization by altering the BM environment through different mechanisms from G-CSF. Notably, a recent study showed that HSPCs could be mobilized from the BM into the circulation by administration of a prostagrandin E_2 (PGE_2) inhibitor, and this effect was independent of CXCL12-CXCR4 signaling [32]. A nucleotide sugar, uridine diphosphate (UDP)-glucose, has also been shown to mobilize subsets of HSPCs functionally distinct from those mobilized by G-CSF, suggesting that UDP-glucose-induced HSPC mobilization would be mediated, at least in part, by different mechanisms from G-CSF [33]. Thus, it would be of interest to examine whether VEGF could influence the levels of BM PGE_2 and/or plasma UDP glucose.

The expression levels of HSC maintenance genes (*Cdh2*, *Vcam-1*, *Angpt1*, and *Thpo*) in BM nonhematopoietic cells were decreased in Ad-VEGF-injected mice (Fig. 3a). This would be due to the reduction in the number of MPCs in the BM after Ad-VEGF injection (Fig. 4). However, we have no idea why BM CXCL12 levels were not changed in Ad-VEGF-injected mice, because MPCs abundantly produce CXCL12 [7,8]. A detailed investigation would be required to clarify the regulation of CXCL12 expression in niche cells, including MPCs, endosteal osteoblasts, and endothelial cells.

We observed enhanced in vitro migration activities of mBMSCs by VEGF, suggesting the possibility that MPCs in the BM would be mobilized to the peripheral tissue in response to the plasma VEGF concentration. However, at present, we did not detect the CFU-F in the blood in Ad-VEGF-injected mice (data not shown). MPCs are known to be rare cells even in the BM, representing $\sim$1 in 10,000–100,000 total nucleated cells [34], and it is therefore possible that the frequency of MPCs in the blood was too low to detect under our experimental conditions. Alternatively, it is also possible that VEGF overexpression in mice might lead to the homing of MPCs to organs, such as the liver, because transgene expression in the liver was extremely high following systemic Ad vector injection [35]. Therefore, it might be necessary to investigate whether or not the frequency and the number of MPCs are changed in tissues or organs other than the peripheral blood.

Recently, Liu et al. showed that MPCs could be mobilized to the peripheral tissue when rats were exposed to hypoxic conditions, and this hypoxia-induced MPC mobilization was caused by the elevation of plasma CXCL12 levels and BM VEGF levels [36]. Under our conditions, however, plasma CXCL12 levels and the BM VEGF levels in Ad-VEGF-injected mice were almost equal to those in Ad-Null-injected mice (Figs. 1b and 3b), suggesting that the mechanisms of decreased number of BM MPCs in Ad-VEGF-injected mice would be different from those of hypoxia-induced MPC mobilization.

Consistent with previous reports [15], we confirmed the HSPC mobilization from BM into the circulation by VEGF overexpression using an Ad vector system (Fig. 1). On the other hand, a previous report showed that administration of a recombinant VEGF protein into mice failed to induce the HSPC mobilization [37]. In our Ad vector systems, plasma VEGF levels were maintained at 400–600 ng/mL on day 3–5 after single intravenous injection. Although we do not know the VEGF levels in the plasma under their experimental protocols, plasma VEGF levels might not be sufficient for HSPC egress from the BM, because exogenous VEGF levels in the plasma were rapidly decreased after administration of a recombinant VEGF protein [23]. Therefore, this difference would be partly due to the difference in the plasma VEGF levels, and we concluded that an Ad vector system would be an appropriate one to estimate the in vivo physiological action of VEGF.

In summary, our results showed that plasma VEGF levels could regulate the distribution of BM HSPCs and MPCs, probably by a mechanism distinct from that of other mobilization factors, and we suggest that a reduction in the number of MPCs in the BM would be one of the mechanisms involved in VEGF-induced HSPC mobilization. Although further investigation of the BM environment will be needed to uncover the VEGF-mediated HSPC mobilization, our findings obtained in this study provide a novel insight into the mechanisms of HSPC mobilization and would be helpful in the development of new clinical mobilizing agents.

Acknowledgments

This work was supported by grants from the Ministry of Health, Labour, and Welfare of Japan, and by the Sasakawa Scientific Research Grant from the Japan Science Society.

Author Disclosure Statement

The authors have no financial conflict of interests.

References

1. Calvi LM, GB Adams, KW Weibrecht, JM Weber, DP Olson, MC Knight, RP Martin, E Schipani, P Divieti, et al.

(2003). Osteoblastic cells regulate the haematopoietic stem cell niche. Nature 425:841–846.
2. Zhang J, C Niu, L Ye, H Huang, X He, WG Tong, J Ross, J Haug, T Johnson, et al. (2003). Identification of the haematopoietic stem cell niche and control of the niche size. Nature 425:836–841.
3. Arai F, A Hirao, M Ohmura, H Sato, S Matsuoka, K Takubo, K Ito, GY Koh and T Suda. (2004). Tie2/angiopoietin-1 signaling regulates hematopoietic stem cell quiescence in the bone marrow niche. Cell 118:149–161.
4. Mendez-Ferrer S, TV Michurina, F Ferraro, AR Mazloom, BD Macarthur, SA Lira, DT Scadden, A Ma'ayan, GN Enikolopov and PS Frenette. (2010). Mesenchymal and haematopoietic stem cells form a unique bone marrow niche. Nature 466:829–834.
5. Omatsu Y, T Sugiyama, H Kohara, G Kondoh, N Fujii, K Kohno and T Nagasawa. (2010). The essential functions of adipo-osteogenic progenitors as the hematopoietic stem and progenitor cell niche. Immunity 33:387–399.
6. Ding L, TL Saunders, G Enikolopov and SJ Morrison. (2012). Endothelial and perivascular cells maintain haematopoietic stem cells. Nature 481:457–462.
7. Ding L and SJ Morrison. (2013). Haematopoietic stem cells and early lymphoid progenitors occupy distinct bone marrow niches. Nature 495:231–235.
8. Greenbaum A, YM Hsu, RB Day, LG Schuettpelz, MJ Christopher, JN Borgerding, T Nagasawa and DC Link. (2013). CXCL12 in early mesenchymal progenitors is required for haematopoietic stem-cell maintenance. Nature 495:227–230.
9. Mendez-Ferrer S, D Lucas, M Battista and PS Frenette. (2008). Haematopoietic stem cell release is regulated by circadian oscillations. Nature 452:442–447.
10. Christopher MJ, F Liu, MJ Hilton, F Long and DC Link. (2009). Suppression of CXCL12 production by bone marrow osteoblasts is a common and critical pathway for cytokine-induced mobilization. Blood 114:1331–1339.
11. Carmeliet P, V Ferreira, G Breier, S Pollefeyt, L Kieckens, M Gertsenstein, M Fahrig, A Vandenhoeck, K Harpal, et al. (1996). Abnormal blood vessel development and lethality in embryos lacking a single VEGF allele. Nature 380:435–439.
12. Ferrara N, K Carver-Moore, H Chen, M Dowd, L Lu, KS O'Shea, L Powell-Braxton, KJ Hillan and MW Moore. (1996). Heterozygous embryonic lethality induced by targeted inactivation of the VEGF gene. Nature 380:439–442.
13. Gerber HP, AK Malik, GP Solar, D Sherman, XH Liang, G Meng, K Hong, JC Marsters and N Ferrara. (2002). VEGF regulates haematopoietic stem cell survival by an internal autocrine loop mechanism. Nature 417:954–958.
14. Chan CK, CC Chen, CA Luppen, JB Kim, AT DeBoer, K Wei, JA Helms, CJ Kuo, DL Kraft and IL Weissman. (2009). Endochondral ossification is required for haematopoietic stem-cell niche formation. Nature 457:490–494.
15. Hattori K, S Dias, B Heissig, NR Hackett, D Lyden, M Tateno, DJ Hicklin, Z Zhu, L Witte, et al. (2001). Vascular endothelial growth factor and angiopoietin-1 stimulate postnatal hematopoiesis by recruitment of vasculogenic and hematopoietic stem cells. J Exp Med 193:1005–1014.
16. Mizuguchi H and MA Kay. (1998). Efficient construction of a recombinant adenovirus vector by an improved *in vitro* ligation method. Hum Gene Ther 9:2577–2583.
17. Mizuguchi H and MA Kay. (1999). A simple method for constructing E1- and E1/E4-deleted recombinant adenoviral vectors. Hum Gene Ther 10:2013–2017.
18. Xu ZL, H Mizuguchi, A Ishii-Watabe, E Uchida, T Mayumi and T Hayakawa. (2001). Optimization of transcriptional regulatory elements for constructing plasmid vectors. Gene 272:149–156.
19. Sakurai H, K Tashiro, K Kawabata, T Yamaguchi, F Sakurai, S Nakagawa, H Mizuguchi. (2008). Adenoviral expression of suppressor of cytokine signaling-1 reduces adenovirus vector-induced innate immune responses. J Immunol 180: 4931–4938.
20. Koizumi N, H Mizuguchi, N Utoguchi, Y Watanabe and T Hayakawa. (2003). Generation of fiber-modified adenovirus vectors containing heterologous peptides in both the HI loop and C terminus of the fiber knob. J Gene Med 5:267–276.
21. Nakamura Y, F Arai, H Iwasaki, K Hosokawa, I Kobayashi, Y Gomei, Y Matsumoto, H Yoshihara and T Suda. (2010). Isolation and characterization of endosteal niche cell populations that regulate hematopoietic stem cells. Blood 116:1422–1432.
22. Okabe M, M Ikawa, K Kominami, T Nakanishi and Y Nishimune. (1997). 'Green mice' as a source of ubiquitous green cells. FEBS Lett 407:313–319.
23. Gabrilovich D, T Ishida, T Oyama, S Ran, V Kravtsov, S Nadaf and DP Carbone. (1998). Vascular endothelial growth factor inhibits the development of dendritic cells and dramatically affects the differentiation of multiple hematopoietic lineages *in vivo*. Blood 92:4150–4166.
24. Sugiyama T, H Kohara, M Noda and T Nagasawa. (2006). Maintenance of the hematopoietic stem cell pool by CXCL12-CXCR4 chemokine signaling in bone marrow stromal cell niches. Immunity 25:977–988.
25. Petit I, M Szyper-Kravitz, A Nagler, M Lahav, A Peled, L Habler, T Ponomaryov, RS Taichman, F Arenzana-Seisdedos, et al. (2002). G-CSF induces stem cell mobilization by decreasing bone marrow SDF-1 and up-regulating CXCR4. Nat Immunol 3:687–694.
26. Ikushima YM, F Arai, K Hosokawa, H Toyama, K Takubo, T Furuyashiki, S Narumiya and T Suda. (2013). Prostaglandin E(2) regulates murine hematopoietic stem/progenitor cells directly via EP4 receptor and indirectly through mesenchymal progenitor cells. Blood 121:1995–2007.
27. Morikawa S, Y Mabuchi, Y Kubota, Y Nagai, K Niibe, E Hiratsu, S Suzuki, C Miyauchi-Hara, N Nagoshi, et al. (2009). Prospective identification, isolation, and systemic transplantation of multipotent mesenchymal stem cells in murine bone marrow. J Exp Med 206:2483–2496.
28. Winkler IG, NA Sims, AR Pettit, V Barbier, B Nowlan, F Helwani, IJ Poulton, N van Rooijen, KA Alexander, LJ Raggatt and JP Levesque. (2010). Bone marrow macrophages maintain hematopoietic stem cell (HSC) niches and their depletion mobilizes HSCs. Blood 116:4815–4828.
29. Levesque JP, J Hendy, Y Takamatsu, PJ Simmons and LJ Bendall. (2003). Disruption of the CXCR4/CXCL12 chemotactic interaction during hematopoietic stem cell mobilization induced by GCSF or cyclophosphamide. J Clin Invest 111:187–196.
30. Brouard N, R Driessen, B Short and PJ Simmons. (2010). G-CSF increases mesenchymal precursor cell numbers in the bone marrow via an indirect mechanism involving osteoclast-mediated bone resorption. Stem Cell Res 5:65–75.
31. Grassinger J, B Williams, GH Olsen, DN Haylock and SK Nilsson. (2012). Granulocyte colony stimulating factor

expands hematopoietic stem cells within the central but not endosteal bone marrow region. Cytokine 58:218–225.
32. Hoggatt J, KS Mohammad, P Singh, AF Hoggatt, BR Chitteti, JM Speth, P Hu, BA Poteat, KN Stilger, et al. (2013). Differential stem- and progenitor-cell trafficking by prostaglandin E2. Nature 495:365–369.
33. Kook S, J Cho, SB Lee and BC Lee. (2013). The nucleotide sugar UDP-glucose mobilizes long-term repopulating primitive hematopoietic cells. J Clin Invest 123:3420–3435.
34. Chamberlain G, J Fox, B Ashton and J Middleton. (2007). Concise review: mesenchymal stem cells: their phenotype, differentiation capacity, immunological features, and potential for homing. Stem Cells 25:2739–2749.
35. Koizumi N, T Yamaguchi, K Kawabata, F Sakurai, T Sasaki, Y Watanabe, T Hayakawa and H Mizuguchi. (2007). Fiber-modified adenovirus vectors decrease liver toxicity through reduced IL-6 production. J Immunol 178:1767–1773.
36. Liu L, Q Yu, J Lin, X Lai, W Cao, K Du, Y Wang, K Wu, Y Hu, et al. (2011). Hypoxia-inducible factor-1alpha is essential for hypoxia-induced mesenchymal stem cell mobilization into the peripheral blood. Stem Cells Dev 20:1961–1971.
37. Pitchford SC, RC Furze, CP Jones, AM Wengner and SM Rankin. (2009). Differential mobilization of subsets of progenitor cells from the bone marrow. Cell Stem Cell 4:62–72.

Address correspondence to:
Dr. Kenji Kawabata
Laboratory of Stem Cell Regulation
National Institute of Biomedical Innovation
7-6-8, Saito-Asagi
Ibaraki, Osaka 567-0085
Japan

E-mail: kawabata@nibio.go.jp

Received for publication September 27, 2013
Accepted after revision December 16, 2013
Prepublished on Liebert Instant Online December 17, 2013

Published online 13 October 2014 *Nucleic Acids Research, 2015, Vol. 43, Database issue* ***D921–D927***
doi: 10.1093/nar/gku955

Open TG-GATEs: a large-scale toxicogenomics database

Yoshinobu Igarashi[1], Noriyuki Nakatsu[1], Tomoya Yamashita[1,2], Atsushi Ono[3], Yasuo Ohno[3], Tetsuro Urushidani[1,4] and Hiroshi Yamada[1,*]

[1]Toxicogenomics Informatics Project, National Institute of Biomedical Innovation, Osaka 567-0085, Japan, [2]Hitachi, Ltd. Information & Telecommunication Systems Company, Government & Public Corporation Information Systems Division, Tokyo 136-8832, Japan, [3]National Institute of Health and Sciences, Tokyo 158-0098, Japan and [4]Department of Pathophysiology, Faculty of Pharmaceutical Sciences, Doshisha Women's College of Liberal Arts, Kyoto 610-0332, Japan

Received August 22, 2014; Revised September 26, 2014; Accepted September 30, 2014

ABSTRACT

Toxicogenomics focuses on assessing the safety of compounds using gene expression profiles. Gene expression signatures from large toxicogenomics databases are expected to perform better than small databases in identifying biomarkers for the prediction and evaluation of drug safety based on a compound's toxicological mechanisms in animal target organs. Over the past 10 years, the Japanese Toxicogenomics Project consortium (TGP) has been developing a large-scale toxicogenomics database consisting of data from 170 compounds (mostly drugs) with the aim of improving and enhancing drug safety assessment. Most of the data generated by the project (e.g. gene expression, pathology, lot number) are freely available to the public via Open TG-GATEs (Toxicogenomics Project-Genomics Assisted Toxicity Evaluation System). Here, we provide a comprehensive overview of the database, including both gene expression data and metadata, with a description of experimental conditions and procedures used to generate the database. Open TG-GATEs is available from http://toxico.nibio.go.jp/english/index.html.

INTRODUCTION

Open Toxicogenomics Project-Genomics Assisted Toxicity Evaluation Systems (TG-GATEs) (Figure 1) is a toxicogenomics database that stores gene expression profiles and traditional toxicological data derived from *in vivo* (rat) and *in vitro* (primary rat hepatocytes, primary human hepatocytes) exposure to 170 compounds at multiple dosages and time points. The toxicology data is composed of biochemistry, hematology and histopathology findings with pathology imaging from the *in vivo* studies and cytotoxicity from the *in vitro* studies. The 170 compounds include representative known liver- and kidney-injuring pharmaceuticals, compounds and chemicals. These data have been generated and analyzed over the course of the 10-year Japanese Toxicogenomics Project (TGP), which was a joint government–private sector project organized by the National Institute of Biomedical Innovation (NIBIO), the National Institute of Health Sciences (NIHS) and 18 pharmaceutical companies (Figure 2).

As specified by relevant regulations, toxicity assessments in the pre-clinical stage of drug development must be conducted using whole animals and cells. In animals, general toxicity in liver and kidney is evaluated with physiological, hematological and biochemical measurements and pathology assessment. In cells, the evaluation of cytotoxicity is conducted by measuring cell viability parameters and morphological changes, often with the use of microscopy. These approaches ensure detection of a certain level of toxicity that might be associated with a given test compound. However, gene expression data is expected to permit the detection of potential toxicities that may not be observable by conventional assessments, thereby facilitating more accurate and predictive decision-making based on toxicity mechanisms (1).

Over the past 10 years, TGP data had been generated at NIHS, NIBIO and several designated contract research organizations using defined standard operating procedures (SOPs). The resulting data were stored, managed and analyzed in a closed version of the database, TG-GATEs. Open TG-GATEs was developed as a publicly available version of the same database, in which the results of 20 118 GeneChip assays are stored along with associated toxicological data and 25 TB of digitized pathology images. Open TG-GATEs is one of the largest public toxicogenomics databases in the world. Using the TG-GATEs data, 36 biomarker sets for specific toxicity mechanisms have to date been defined dur-

*To whom correspondence should be addressed. Tel: +81 72 641 9826; Fax: +81 72 641 9850; Email: h-yamada@nibio.go.jp

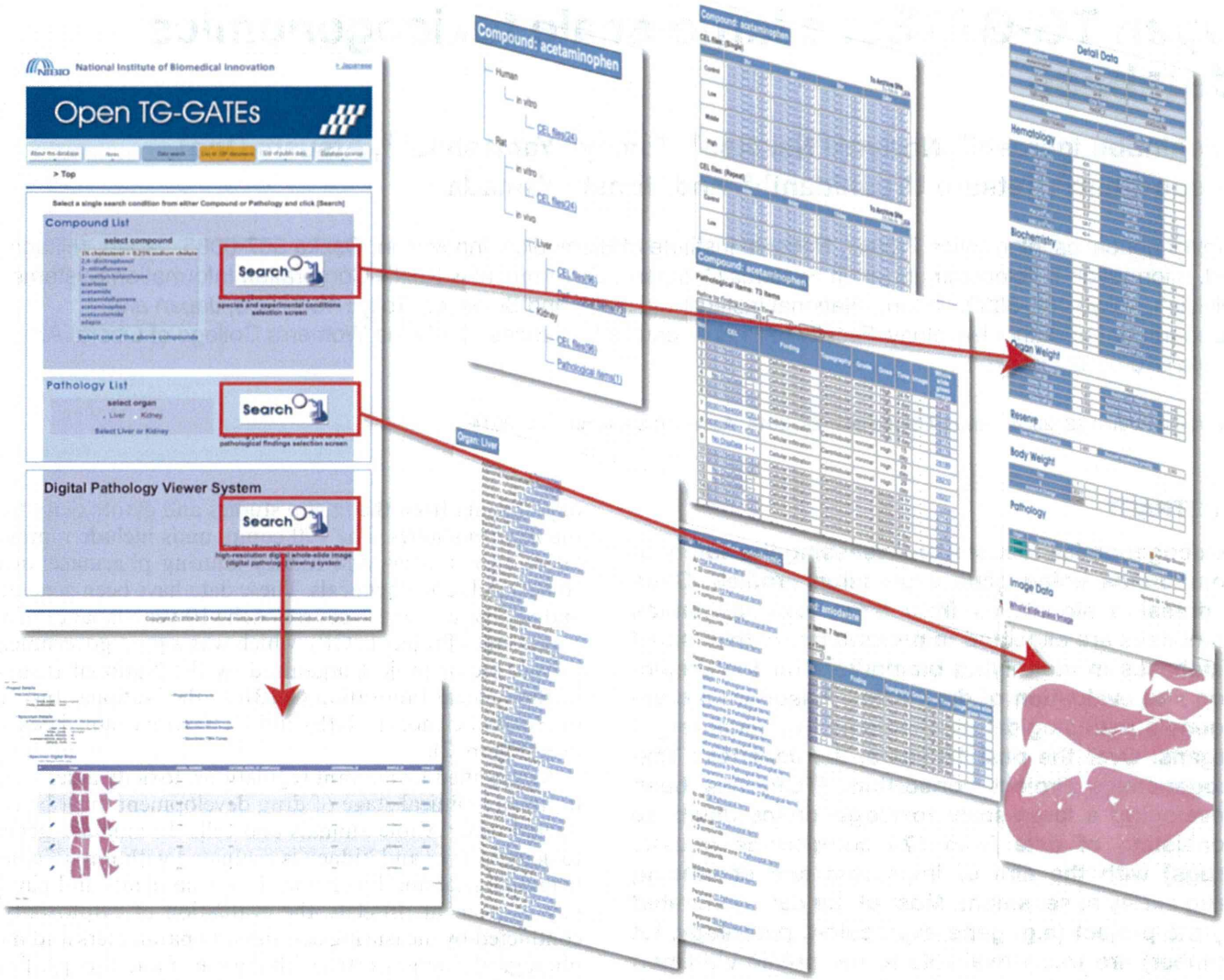

Figure 1. Open TG-GATEs offers hierarchical access from compound and pathology lists to hematology, biochemical parameters and digitized pathology images. Gene expression data are stored as CEL files, which require software capable of interacting with the Affymetrix data file format. Thus, users will have to convert the primary data into a general-purpose format using various algorithms such as MAS5.0, RMA, etc.

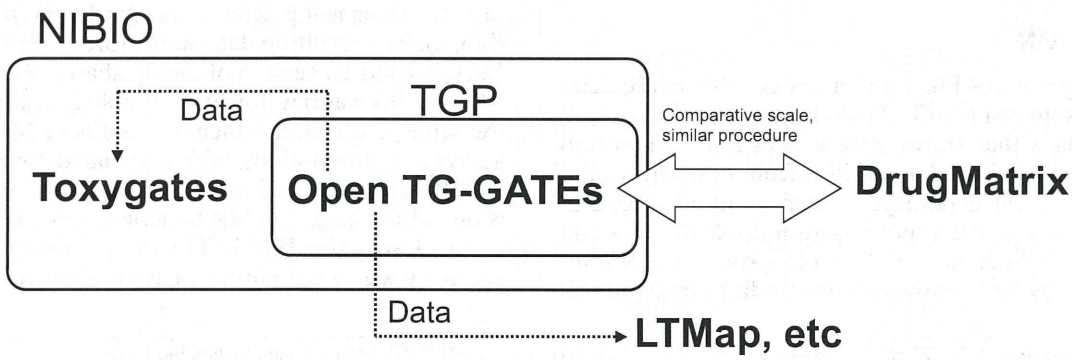

Figure 2. The relationship of the databases and organizations are shown. The dotted line shows the data distribution. NIBIO: National Institute of Biomedical Innovation, TGP: Toxicogenomics project in Japan.